5th International Conference
"Computational Mechanics and Virtual Engineering"
COMEC 2013
24- 25 October 2013, Braşov, Romania

COMPARATIVE ANALYSIS OF THE CRACKING RATE FOR A STAINLESS STEEL LOADED AT 213K TEMPERATURE

Roşca, V.[1], Miriţoiu, C.[1], Geonea, I.[1], Romanescu, Alina[1]
[1] Mechanics Faculty, University of Craiova, Romania, rosca_valcu@yahoo.com

Abstract: *The existance of a variable (cyclic) loading over a part or an subassembly may lead to the crack appearance in its body. The crack will spread unit it will reach a critical length leading to the instant specimen fracture. An important parameter that can control the fatigue fracture is the* ***crack propagation rate*** *marked as* ***da/dN****. This is the advancing length of the crack in a loading cycle. There were proposed, by various scientists from the researching field, many empiric relations, that have resulted from the experiments, that follow the fatigue fracture phenomena. In this paper a comparative analysis of the cracking speed will be made by using three mathematical models: Paris formula, Walker relation and Donahue relation. The experiments were made on CT specimens, with side notch, from a stainless steel 10TiNiCr175 type. The loading* ***temperature*** *was* ***213K*** *(meaning -60°C), and the loading was made for three types of asymmetry factors:* ***R=0.1****,* ***R=0.3*** *and* ***R=0.5****. During the loadings, some primal quantities were take into account: the variation of the cracking length* a_i *and the corresponding cycles number* N_i*. With these values there was calculated the variation of an important parameter in the* ***Fracture Mechanics****,* ***ΔK– the stress intensity factor*** *, and respectively the* ***crack growth rate da/dN*** *by polynomial method and the three presented models. With the obtained models some graphics were drawn representing the* ***da/dN*** *parameter variation and there were made comparisons between the four used formulas.*
Keywords: *crack, fracture, stress intensity factor, crack growth rate, asymmetry coefficient*

1. INTRODUCTION

Some products or parts that are included in the composition of some equipments or aggregates from the chemical, food or extractive industry work in low temperature or cryogenic environments. The used materials must have a good behavior at these temperatures, must not modify their physical-mechanical properties during their activity. That is why it is necessary to permanently follow their structural integrity.
A material used to design these parts is the 10TiNiCr175 stainless steel, V2A class. Beside the working environment temperature, a considerable influence over the material strength is the loading type: static, dynamic and variable character. In this last case of loading, the loading degree is very important, namely the loading asymmetry factor **R**, ie $R= \sigma_{min}/\sigma_{max}$, where σ_{min} and σ_{max} represent the minimum and maximum stresses, where the stress state varies.
During the working time, because of some material, constructive, environment or loading factors, micro-cracks may appear which can increase up to a critical value producing the final fracture of the product.
In addition to the "Strength of Materials" classical calculus, there can be made a complex analysis of the materials breaking state using the notions from "Fracture Mechanics".
The main parts that control the material facture process of a fatigue loaded product are the **cracking rate** marked with **da/dN** or **da/dt** and the **stress intensity factor variation** marked with **ΔK** [1], [6]. We mark with: **a** is the crack length, **N** is the loading cycle number and by **t** is marked the reference time, at which the crack variation **da** is reported. A general calculus relation for the stress intensity factor, abbreviated with **SIF**, it is founded in many references and has the form of relation (1) [6], 3.6 formula/pp. 32:

$$\Delta K = C \cdot \Delta\sigma \cdot \sqrt{a} \,. \tag{1}$$

We can see that this relation simultaneously included the loading stress **σ** and the crack length **a**, and **C** is a parameter that can be determined by using many relations, being dependent on the crack domain and geometry.
An important graphic of the cracking rate variation **da/dN** in relation with the stress intensity factor variation **ΔK** is presented in figure 1, [3], [4], [6]. In this graphic we can distinguish three domains:
- I – the crack initiation domain;
- II - the area of the crack stable propagation, which can be controlled and followed;

- III – brutal and fragile cracking domain, which cannot be controlled.
There are highlighted two very important values for SIF: threshold stress intensity factor ΔK_{th}, respectively the critical stress intensity factor or the fracture tenacity K_c, figure 1.

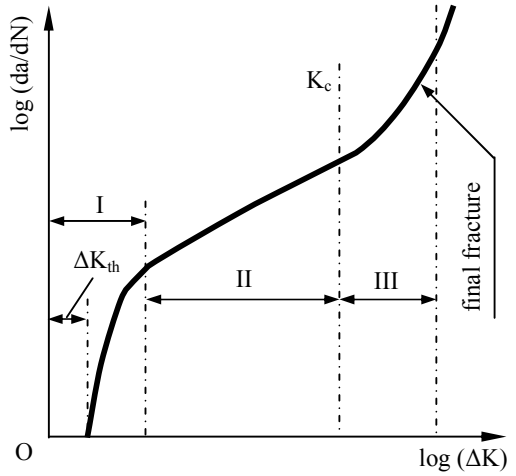

Figure 1: Cracking Rate Versus Stress Intensity Factor
(bilogarithmically coordinates)

In order to determine the propagation cracking speed, **da/dN**, some researchers have presented several empirical formulas that have resulted from experimental data. Mostly target the second domain of the sigmoid curve, figure 1. For our paper we have limited at the analysis of four studying models, marked in this way:
- 1 - the sequential polynomial method according to the ASTM E647 standard [7], [4], [6];
- 2- Paris P.C.formula, [3]- pp. 204, [6]-pp.42;
- 3- Walker K. formula [3]- pp.209;
- 4- Donahue J.R. formula [3]- pp. 209.
For the models presented above, the mathematical calculus relations for the propagation cracking rate are:

- Paris formula: $\frac{da}{dN} = V_2 = C_2 \cdot (\Delta K)^{m_2}$; (2)

- Walker formula: $\frac{da}{dN} = V_3 = C_3 \cdot \frac{(\Delta K)^{m_3}}{(1-R)^{r_3}}$; (3)

- Donahue formula: $\frac{da}{dN} = V_4 = C_4 \cdot (\Delta K - \Delta K_{th})^{m_4}$. (4)

The factors C_2, m_2, C_3, m_3, C_4, m_4 and r_3 are material constants and are obtained at the experimental data processing inserting the condition that a part from the second domain, figure 1, to be successively approximated with the (2), (3) and (4) relations.

2. EXPERIMENTS AND RESULTS PROCESSING

From a bar strip, made by 10TiNiCr175 stainless steel, several CT type C-R model specimens were processed, with side notch, figure 5.3, pp. 86/ [4]. The same loading force is applied on circumferential direction and the crack propagation takes place on the radius R direction, figure 5.7/ pp. 89/ [4]. The specimens were tested on a hydraulic pulsing device, with a freezing chamber, figure 5.8/pp. 92/ [4], [5]. The testing temperature was **213K** (-60°C) and there were used three asymmetry factors: **R=0.1**, **R=0.3** and **R=0.5**, meaning eccentrical tensile fatigue loadings, positive oscillating. During the loading, after a first-crack in which the threshold stress intensity factor ΔK_{th} was achieved, that corresponds to the crack length a_0, it was passed in the stable propagation domain (II) and it was marked successively the crack length variation a_i, respectively the number of the loading cycles N_i. For the crack length calculus an extensometer with elastic lamellae was used, figure 5.12/ pp.97/ [4], [5] with a results conversion using the elastic compliance method [2], pp. 862-873, [4], pp. 96.

The values sets ($\mathbf{a_i}$, $\mathbf{N_i}$) experimentally obtained are processed using **the sequential polynomial method** according to the **ASTM E-647** standard: [4]- pp.82, [6]- pp.146, [7], determining the growth cracking rate with the formula 4.10/pp.83/[4]:

$$\frac{da}{dN} = V_1 = \frac{A_1}{C_2} + 2 \cdot A_2 \cdot \frac{N_i - C_1}{C_2^2}, \tag{5}$$

(see relations (2), (3), (4)/[5])

Then, there will be determined the stress intensity factor variation **ΔK** for any value of the crack length $\mathbf{a_i}$: [3]/pp.66, [5]/ pp.83, [6]/pp.146,

$$\Delta K = \frac{\Delta F}{B\sqrt{W}} \cdot \frac{2 + \frac{a}{W}}{\left(1 - \frac{a}{W}\right)^{\frac{3}{2}}} \cdot \left[-5{,}6 \cdot \left(\frac{a}{W}\right)^4 + 14{,}72\left(\frac{a}{W}\right)^3 - 13{,}32\left(\frac{a}{W}\right)^2 + 4{,}64\frac{a}{W} + 0{,}886 \right], \tag{6}$$

where: ΔF- is the loading force variation, in N;

B- is the specimen thickness, in mm;

W- is the specimen active width, in mm.

It is continuously followed an elastic loading using the condition a/W≥ 0,2 , and ΔK will result in [N·mm$^{-3/2}$].

Complying the methodology presented in the introduction, there will be determined the speeds V_2, V_3 and V_4. With the obtained values, there will be drawn the next curves:

- the cracking rates $\mathbf{V_1}$, $\mathbf{V_2}$, $\mathbf{V_3}$ and $\mathbf{V_4}$ in relation with the crack length variation **a**, for the asymmetry factor **R=0.1**, in the same graphic, figure 2;
- the same thing for **R=0.3**, figure 3;
- the same thing for **R=0.5**, figure 4;
- the propagation cracking rates $\mathbf{V_1}$, $\mathbf{V_2}$, $\mathbf{V_3}$ and $\mathbf{V_4}$ in relation with the stress intensity factor **ΔK**, for the asymmetry factor **R=0.1**, on the same graphic, figure 5;
- the same thing for **R=0.3**, figure 6;
- the same thing for **R=0.5**, figure 7;
- $\mathbf{V_1}$ speed, according to the ASTM E-647 standard, in relation with the crack length variation **a**, for the three asymmetry factors (**R=0.1, R=0.3** and **R=0.5**), on the same graphic, figure 8;
- $\mathbf{V_1}$ speed versus SIF **ΔK** variation, for the three asymmetry factors, simultaneously, figure 9.

3. COMMENTS. OBSERVATIONS

After a general analysis of the cracking variation rates curves according to the four variants versus the crack length variation **a**, and versus SIF variation **ΔK**, it can be said that on the area of the crack stable propagation (second domain – figure 1), the empirical models used in this paper approximate very well the fracture phenomenon.

For the asymmetry factor **R=0.1**, the crack evolution **a** is analyzed from 10,75 mm up to 15,5 mm, where the propagation is in the linear-elastic limits and the cracking rates vary from 118,9·10^{-6} m/cycle , for $\mathbf{V_1}$, up to 470,03·10^{-6} m/cycle for Walker model ,$\mathbf{V_3}$, figure 2. Reported to SIF, for the same cracking rates domain, the **KΔ** factor variation is in the limits of: 776 Nmm$^{-3/2}$ up to 1170 Nmm$^{-3/2}$, when it is obtained the breaking tenacity (K_c= 1170 Nmm$^{-3/2}$), figure 5.

By analyzing the loading factor **R=0.3**, the crack length varies between 11,25 mm and 15,75 mm, and the speeds domain ranges between 22,4·10^{-6} m/cycle and 152,7·10^{-6} m/cycle, figure 3 and figure 6. According to these limits, the **ΔK** SIF variation is produced between 632 Nmm$^{-3/2}$ and 934 Nmm$^{-3/2}$, figure 6. There can be noticed that, at the beginning of the second domain, the propagation according to the **Donahue model** is more slowly, and in the second part, according to the **Walker model**, the propagation is more quickly, figure 3 and figure 6.

The asymmetry factor **R=0.5** is placed for crack lengths between 10,75 mm and 13,5 mm. The crack rates increasing domain ($\mathbf{V_1}$, $\mathbf{V_2}$, $\mathbf{V_3}$ and $\mathbf{V_4}$) vary between 26,9·10^{-6} m/cycle by polynomial method ($\mathbf{V_1}$) and 55,2·10^{-6} m/cycle for the Paris model ($\mathbf{V_2}$). Accordingly, the stress intensity factor **ΔK** increase from 428 Nmm$^{-3/2}$ up to 532 Nmm$^{-3/2}$. In this case, slope variation curves of **da/dN** crack growth rate is lower than the previous cases, figure 4 and figure 7.

About the figure 8 and figure 9, there was presented only the $\mathbf{V_1}$ rate variation versus the crack length **a**, figure 8, respectively versus **ΔK** SIF, figure 9, for the three asymmetry factors **R=0.1, R=0.3** and **R=0.5**, simultaneously. It is observed that an increase of the **R** factor leads to a decrease of the $\mathbf{V_1}$ cracking rate, figure 8, and in the same time a decrease of the **ΔK** SIF variation, figure 9. Variation limits for the **a** lengths, **ΔK** factors and $\mathbf{V_1}$ length were remembered above.

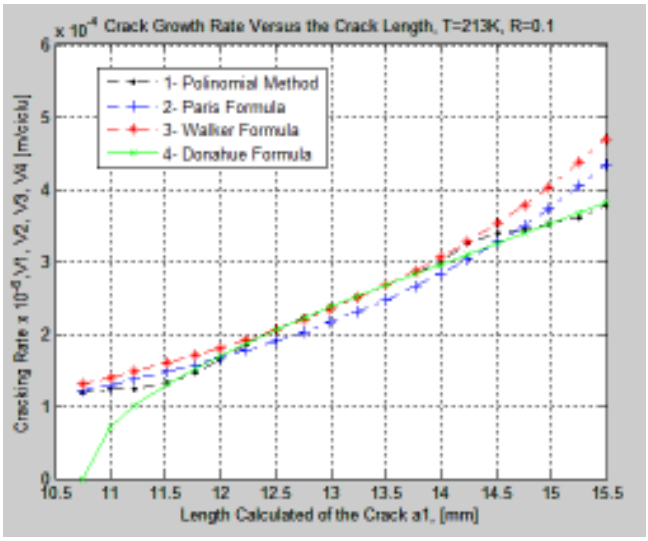

Figure 2: Crack Growth Rates Versus the Crack Length for R=0,1

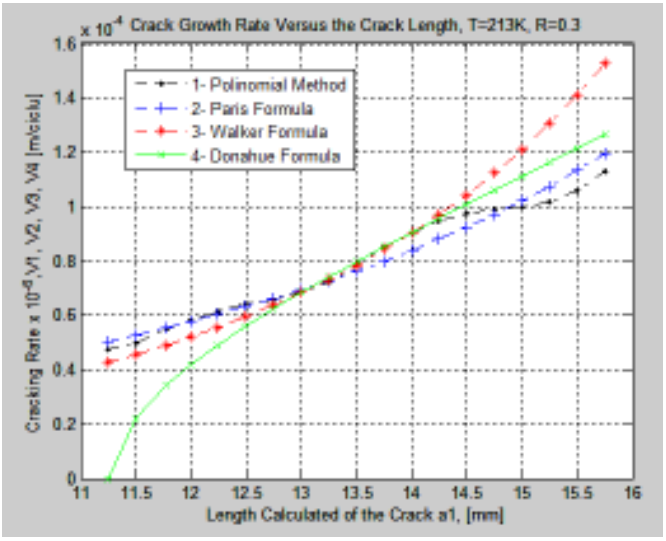

Figure 3: Crack Growth Rates Versus the Crack Length for R=0,3

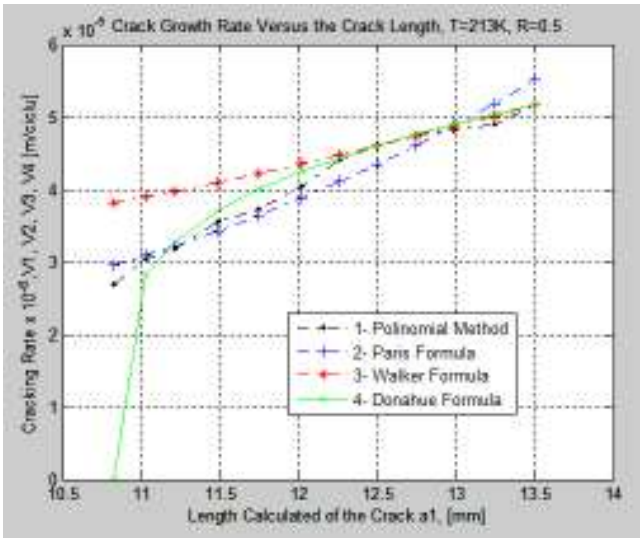

Figure 4: Crack Growth Rates Versus the Crack Length for R=0,5

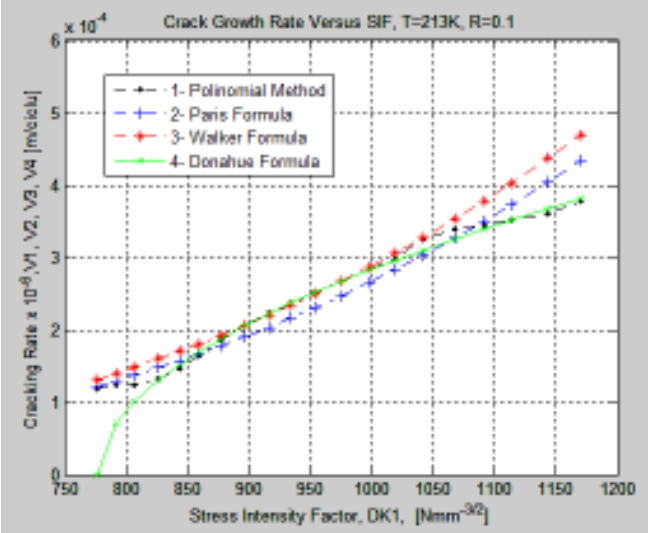

Figure5: Crack Growth Rates Versus SIF for R=0,1

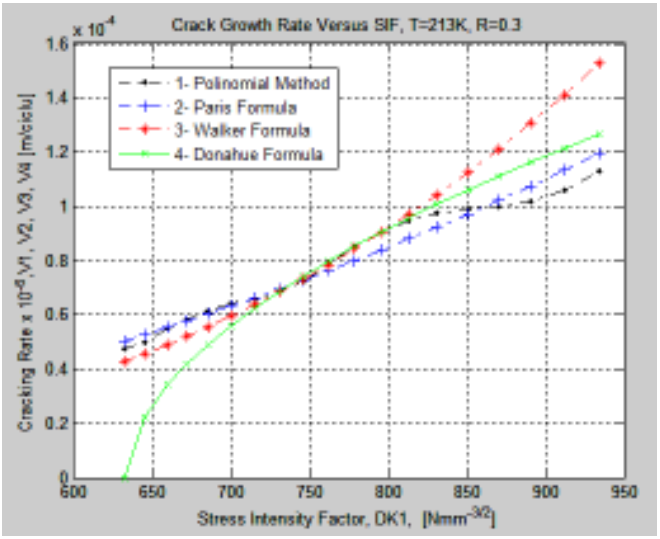

Figure 6: Crack Growth Rates Versus SIF for R=0,3

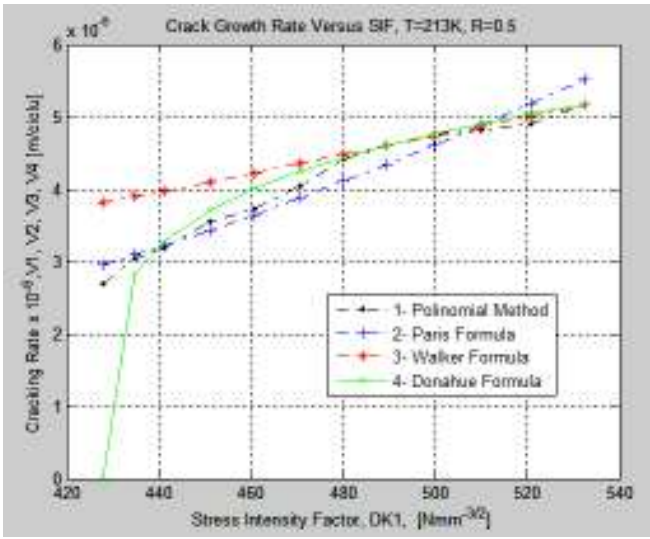

Figure 7: Crack Growth Rates Versus SIF for R=0,5

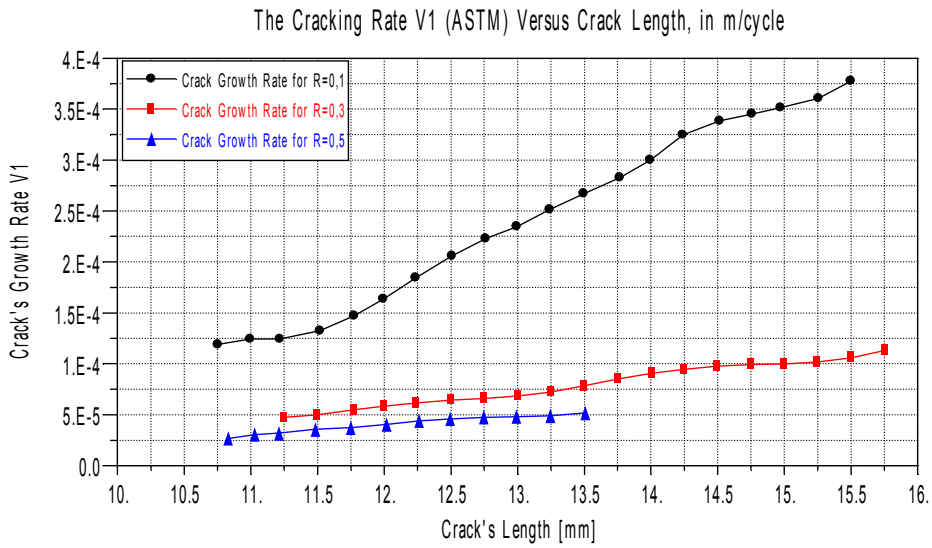

Figure 8: Crack Growth Rate **V1** (ASTM) Versus Crack's Length **a**

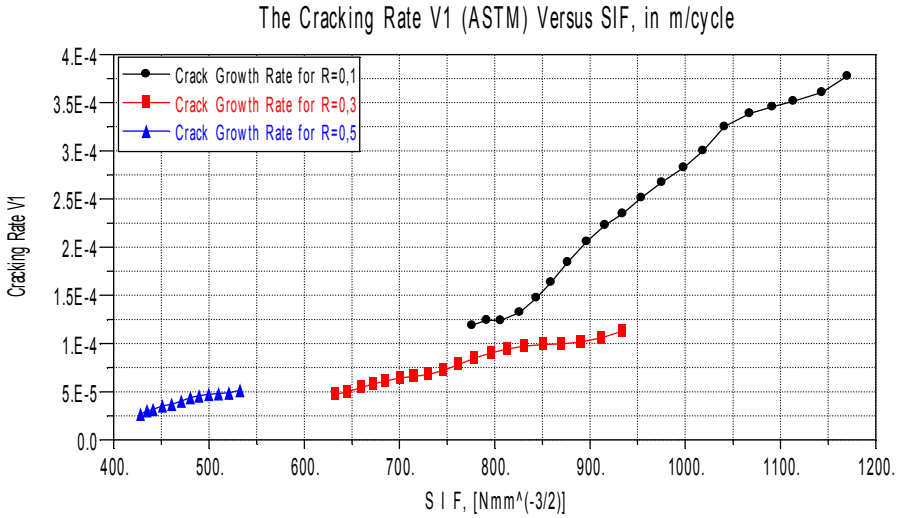

Figure 9: Crack Growth Rate **V1** (ASTM) Versus SIF **ΔK**

REFERENCES

[1] Dumitru, I., Bazele Calculului la Oboseală, Editura Eurostampa, Timişoara, 2009;

[2] Mc Henry, H.I., A Compliance Method for Crack Growth Studies at Elevated Temperatures, Journal of Materials, Tom 6, Nr.4, December, 1971, p.862-873;

[3] Pană, T., Pastramă, St., D., Integritatea Structurilor Mecanice, Editura Fair Partners, Bucureşti, 2000;

[4] Roşca, V., Contribuţii la Studiul Oboselii Monoaxiale la Temperaturi Scăzute, Teză de Doctorat, Universitatea Politehnica Bucureşti, 1997;

[5] Roşca, V., Miriţoiu, C., Geonea, I., Romanescu, Alina, Empiric Models for Study the Crack Increase Speed in Steel R520, International Conference of Mechanical Engineering, ICOME 2013, Craiova, Romania, Tom.I, Universitaria Publishing House, p.273-280;

[6] Rusu, O., Teodorescu, M., Lascu-Simion, N., Oboseala Metalelor, vol. 1- Baze de calcul, vol. 2 – Aplicaţii inginereşti, Editura Tehnică, Bucureşti, 1992;

[7] ASTM E-647-95 Standard Test Method for Measurement of Fatigue Crack Growth Rates, American National Standard.